

This discussion paper is/has been under review for the journal Biogeosciences (BG).
Please refer to the corresponding final paper in BG if available.

Detection of wetland dynamics with ENVISAT ASAR in support of methane modelling at high latitudes

**A. Bartsch¹, A. M. Trofaier², G. Hayman³, D. Sabel¹, S. Schlaffer¹, D. Clark³, and
E. Blyth³**

¹Vienna University of Technology, Institute of Photogrammetry and Remote Sensing,
1040 Vienna, Austria

²Scott Polar Research Institute, University of Cambridge, Cambridge, CB2 1ER, UK

³Centre for Ecology and Hydrology, Wallingford, Oxfordshire, OX10 8BB, UK

Received: 22 July 2011 – Accepted: 8 August 2011 – Published: 12 August 2011

Correspondence to: A. Bartsch (annett.bartsch@tuwien.ac.at)

Published by Copernicus Publications on behalf of the European Geosciences Union.

BGD

8, 8241–8268, 2011

High latitude wetland dynamics

A. Bartsch et al.

Title Page

Abstract

Introduction

Conclusions

References

Tables

Figures

◀

▶

◀

▶

Back

Close

Full Screen / Esc

Printer-friendly Version

Interactive Discussion



Abstract

Spatial information on inundation dynamics is expected to improve greenhouse gas estimates in climate models. Satellite data can provide land cover information from local to global scale. The detection capability for dynamics is however limited. Cloud cover and daylight independent methods are required for frequent updates. Suitable are therefore sensors which make use of microwaves. The purpose of the present study is to assess such data for determination of wetland dynamics from the viewpoint of use in climate models of the boreal and tundra environments. The focus is on synthetic aperture radar (SAR) operating in C-band due to, among microwave systems, comparably good spatial resolution and data availability. Continuity is also expected for such systems. Simple classification algorithms can be applied to detect open water in an automatised way allowing the processing of time series. Such approaches are robust when the water surface is smooth. C-band data from ENVISAT ASAR (Advanced SAR) operating in wide swath mode (150 m resolution) have been investigated for implementation of an automated detection procedure of open water fraction. More than 4000 samples (single acquisitions tiled into 0.5 degree grid cells) have been analysed for July/August 2007 and 2008. Modification of input parameters results in differences below 1 % open water fraction. The actual challenge is the frequent occurrence of waves due to wind and precipitation. This reduces the separability of the water class from other land cover. The possible update intervals for surface water extent are therefore decreased considerably. Statistical measures of the backscatter distribution can be applied in order to retrieve the for classification suitable data. The Pearson correlation between each sample dataset and a location specific representation of the bimodal distribution has been used for assessment. On average only 40 % of acquisitions allow a separation of the open water class. Satellite data are available every 2–3 days over the Western Siberian study region. With respect to the irregular acquisition intervals and varying length of unsuitable weather periods a minimum update interval of 10 days is suggested for the Northern Eurasian test case. Although SAR data availability is currently constraint future satellite missions which aim for operational services such

High latitude wetland dynamics

A. Bartsch et al.

Title Page

Abstract

Introduction

Conclusions

References

Tables

Figures



Back

Close

Full Screen / Esc

Printer-friendly Version

Interactive Discussion



as Sentinel-1 with its C-band SAR instrument may provide the basis for inundation monitoring in support of climate modelling.

1 Introduction

The global annual source strength of CH₄ is relatively well constrained (Denman et al., 2007), although considerable uncertainties exist in the partitioning of sources and their spatial and temporal distribution. Wetlands are generally accepted as being the largest but least well quantified single source of CH₄, ranging from 100 Tg yr⁻¹ (Wuebbles and Hayhoe, 2002) to 231 Tg yr⁻¹ (Mikaloff Fletcher et al., 2004). Northern high latitude wetland ecosystems are of particular importance due to their potential for turning from a carbon sink to a net carbon source. Large parts are underlain by perennially frozen ground. A total 1672 petagrams of soil carbon is estimated to be stored in northern permafrost regions (Schuur et al., 2008). Emissions of methane from the wetlands and lakes of the Boreal region contribute much less than the tropical wetlands to the global wetland methane emissions: Walter et al. (2001) calculate that only 25 % of the wetlands emissions come from wetlands north of 30° North. However, due to the increased warming expected over the northern latitudes, they are likely to change more than the emissions from tropical regions.

There is much current interest in modelling methane emissions from wetlands and peatlands on the regional and global scales (e.g. Wania et al., 2009a,b; Petrescu et al., 2010; Ringeval et al., 2010, 2011; Riley et al., 2011). Riley et al. (2011) present an overview of the various biogeochemical processes involved in methane generation and the challenges of representing these processes in large-scale model applications. These (e.g. Ringeval et al., 2010, 2011) and other similar land surface models (e.g. JULES, the Joint UK Land Earth Simulator, Clark et al., 2011) typically operate at 0.5°/1.0° or larger spatial resolution and use relatively simple methane wetland emission parameterisations based on the main controls of temperature, wetland fraction and substrate availability.

BGD

8, 8241–8268, 2011

High latitude wetland dynamics

A. Bartsch et al.

Title Page

Abstract

Introduction

Conclusions

References

Tables

Figures

◀

▶

◀

▶

Back

Close

Full Screen / Esc

Printer-friendly Version

Interactive Discussion



The wetland maps of Matthews and Fung (1987) and Lehner and Döll (2004) have been much used to represent wetlands. These datasets provide global information on wetland extent and types but do not include dynamics. Satellite data have been shown of large value for wetland monitoring. The applications range from identification of aquatic vegetation to inundation dynamics. Different type of sensors can be employed at varying scales. Continental to global monitoring requires a specific acquisition strategy. This includes regular coverage at as short as possible intervals. Spatial detail always goes to the expense of sampling intervals. Best sampling offer microwave sensors which are cloud and illumination independent. Passive as well as active microwave sensors have been shown to be applicable. Passive (SSM/I) and active microwave (ERS C-band scatterometer) information has been combined with medium resolution optical data (AVHRR) for a global representation of dynamics (Prigent et al., 2001, 2007). A combination of a Ku-Band scatterometer (Seawinds on QuikScat) and a passive instrument (AMSR-E) has been shown suitable for detection of dynamics over Siberia (Schroeder et al., 2010). Seawinds provided ten years of global data coverage but stopped operation in 2009 (Bartsch, 2010). The information retrieved from these global data is rather coarse with >25 km resolution. However, since inundation fraction is reported, this resolution represents sufficient grid spacing with respect to climate modelling. Such data may be therefore applied for improvement of methane modelling.

Both Ringeval et al. (2010, 2011) and Riley et al. (2011) have based the modeled wetland fraction on the global Earth Observation product of Prigent et al. (2007), which gives the area of inundation on a monthly timescale. As highlighted by Riley et al. (2011), Prigent et al. (2007) acknowledged that their product may not capture small, isolated water bodies in areas that are otherwise largely unsaturated (i.e. small fractional inundations of less than 10% cover).

Medium resolution satellite data which are used for land cover maps (such as from MODIS, 500 m) show in general low accuracy in high latitude environments, since e.g. tundra ponds are mostly below the resolution of the satellite data (Bartsch et al., 2008; Frey and Smith, 2007). Synthetic aperture radars (SARs) operating in ScanSAR

BGD

8, 8241–8268, 2011

High latitude wetland dynamics

A. Bartsch et al.

Title Page

Abstract

Introduction

Conclusions

References

Tables

Figures

◀

▶

◀

▶

Back

Close

Full Screen / Esc

Printer-friendly Version

Interactive Discussion



mode (e.g. ENVISAT ASAR Wide Swath, 150 m) have shown to be applicable for efficient and accurate water bodies mapping at high latitudes (Bartsch et al., 2008).

The clear advantage of using SAR is its capability of resolving the smaller water bodies. Further, this provides a dataset to validate global products. From a modelling perspective, the high resolution product ideally needs to be complete in space and time for the domain of interest. The question is whether ScanSAR data which exist in archives are suitable for mapping of dynamics in tundra as well as boreal environments. Issues which need to be considered are the typically irregular acquisition intervals, constraints of the used frequency, classification method and data management issues which arise with the chosen resolution and location of the area of interest. This has been investigated with ENVISAT ASAR wide swath data over a selected site of northern Eurasia. Uncertainties are quantified and discussed with respect to use in climate models and future satellite data availability.

2 Material and methods

Permanent and seasonal inundation are surface phenomena which can be easily mapped by means of active microwave sensors. The incident radar beam is reflected off smooth water surfaces away from the sensor. This specular reflection results in low backscatter values which are hence associated with water pixels (e.g. applied in Bartsch et al., 2008; Matgen et al., 2011). This behavior is very distinct from other land cover; low backscatter may however also be the result of melting snow surface and ice or radar shadow caused by steep terrain and side-looking sensors. Wave action increases the roughness and thus backscatter to the level of the surrounding land cover depending on wavelength. The majority of SAR data available for civil use to date is acquired by C-band instruments (ERS, Radarsat, ENVISAT ASAR). Continuation of records are ensured due to future plans of the European Space Agency with the Sentinel satellites series (Attema et al., 2007). This makes such kind of sensors interesting

BGD

8, 8241–8268, 2011

High latitude wetland dynamics

A. Bartsch et al.

Title Page

Abstract

Introduction

Conclusions

References

Tables

Figures

◀

▶

◀

▶

Back

Close

Full Screen / Esc

Printer-friendly Version

Interactive Discussion



High latitude wetland dynamicsA. Bartsch et al.

[Title Page](#)[Abstract](#)[Introduction](#)[Conclusions](#)[References](#)[Tables](#)[Figures](#)[◀](#)[▶](#)[◀](#)[▶](#)[Back](#)[Close](#)[Full Screen / Esc](#)[Printer-friendly Version](#)[Interactive Discussion](#)

for especially climate research which requires longterm records. The wavelength is between 5–6 cm. Already slight wind action can therefore impede the specular reflection. Longer wavelengths such as L-band (>20 cm) are more suitable but availability is limited at present as well as in the near future. A further problem which is induced by the wavelength is the penetration of the signal through emerging vegetation. Especially lake shores can be affected. When open water starts to freeze up backscatter also increases considerably (e.g. Duguay et al., 2002).

Inundation is expected to occur over flat terrain. The region of specific interest for this study are the West Siberian lowlands (WSL, test region of the ESA STSE ALANIS-Methane project, <http://www.alanis-methane.info>), where in case of spaceborne remote sensing radar shadow is not expected. This region also lies outside of glaciated terrain. The similarity of the backscatter return to melting seasonal snow and different backscatter behavior of lakes in winter need, however to be accounted for. This can be achieved by usage of auxiliary data (e.g. Bartsch et al., 2009). For the purpose of this study the analyses period has been confined to summer, July to August. Data from two consecutive years 2007 and 2008 have been analysed.

The region which has been investigated for this study is a transect within the West Siberian Lowland spanning from 68–73° East and 63–69° North. It has been selected due to data availability (see Fig. 1) and it also covers part of the largest peatland of the world (Keddy and Fraser, 2005). Atmospheric methane variations over the summer from year to year have been reported from ENVISAT SCIAMACHY data for this region (Schneising et al., 2011). The area excludes large parts of the Ob River and its floodplain. Water fraction is expected to vary for large rivers with respect to wave action. Flooded river valleys are also suggested to be excluded for the purpose of methane modelling (Ringeval et al., 2010). The focus is therefore instead on changes over other areas but nevertheless also a part of the Ob River floodplain is included.

In a first step the previously tested method of simple thresholding (Bartsch et al., 2008) is applied for the different environments. The region comprises the boreal peatland as well as tundra with thermokarst ponds. The applicability of a universal threshold

is tested with a sensitivity analyses. The problem of wave action is specifically addressed by time series analyses and comparison with meteorological data.

2.1 ENVISAT ASAR Wide Swath data

The Advanced Synthetic Aperture Radar (ASAR) instrument onboard the European Space Agency's (ESA) ENVISAT platform is a C-Band (centre frequency at 5.331 GHz) sensor that can operate in different modes of varying spatial and temporal resolution. In Wide Swath mode (WS) the instrument has a spatial resolution of 150 m.

WS data are only acquired on request, restricting their availability in general to archived material. Figure 1 shows the data coverage for higher latitudes of the Northern Hemisphere. Data are almost exclusively taken in HH (horizontal emitted and horizontal received) polarisation. A minimum of five acquisitions per month have been acquired in the summers 2007 and 2008 over the studied region.

The ENVISAT ASAR WS data are distributed via the ESA rolling archive in Level 1b. These data require preprocessing before the actual wetland classification can be made. This is done using the IPF's SAR Geophysical Retrieval Toolbox (SGRT), which is an in-house developed scripting chain that calls the commercially available SARscape or the free NEST software, allowing for the automatisation of the entire preprocessing procedure. Radiometric calibration and geocoding follow the Range-Doppler approach. The backscatter coefficient (σ^0) is modelled as a function of the local incidence angle and is expressed in units of decibel (dB). The ASAR WS data are adjusted to a reference incidence angle of 30° (Sabel et al., 2011).

The northern location of the transect and the high amount of data needs to be taken into consideration for the processing and database setup. All data are geocoded to a polar stereographic projection in order to avoid oversampling and reduce storage needs. The used projection is of the conformal conic type and is e.g. used by the National Snow and Ice Data Center (NSIDC) in the United States for polar datasets.

BGD

8, 8241–8268, 2011

High latitude wetland dynamics

A. Bartsch et al.

Title Page

Abstract

Introduction

Conclusions

References

Tables

Figures

◀

▶

◀

▶

Back

Close

Full Screen / Esc

Printer-friendly Version

Interactive Discussion



Water fraction is eventually extracted with respect to climate model grid cells. Only data from scenes which cover a complete 0.5 degree grid cell are considered for further analyses. The classification results are aggregated for this grid size.

2.2 Inundation mapping

5 The backscatter value distribution of a SAR image over lake abundant terrain is of a bimodal nature. This is the result of diffusive (surroundings) and specular (water bodies) reflection; diffusive scatter being the dominant mode if the water fraction is below approximately 50 % what is expected over the region of interest. Therefore a straight forward classification procedure for open water mapping can be established by setting a simple threshold value. Any normalized backscatter value that falls below this threshold is attributed to specular reflection and hence is classified as water. Alternative methods also consider flooding below vegetation, what can be achieved by using L-band SAR data and optical data consider e.g. the random forest approach (Schroeder et al., 2010; Whitcomb et al., 2009). Variations in the maximum of the water peak and minimum between the peaks for the same region can occur due to the changing roughness of the water. Adaptive approaches describe the mode (backscatter distribution) of water as Gamma distributed (Matgen et al., 2011) which can serve as input for classification algorithms. The overlap of the two modes/landcover types (larger values than threshold) can then be integrated via region growing.

15 The threshold value which lies between the modes has been found to be at approximately -14 dB in the case of normalization of σ_0 to 30° in tundra (Bartsch et al., 2009). This value is tested in the automated classification procedure. A Gaussian function was fit to the backscatter value distribution for further description of the empirically determined threshold. It is approximately within 3σ of the mean of the dominant mode. Figure 2a shows a normalized image scene and histogram of the WS data. The water bodies can be clearly distinguished from their surroundings. In this case $\mu_{dm} - 3\sigma_{dm} = -14.4$ dB, where μ_{dm} and σ_{dm} are the mean and the standard deviation of the dominant mode, respectively.

High latitude wetland dynamics

A. Bartsch et al.

Title Page

Abstract

Introduction

Conclusions

References

Tables

Figures

◀

▶

◀

▶

Back

Close

Full Screen / Esc

Printer-friendly Version

Interactive Discussion



High latitude wetland dynamics

A. Bartsch et al.

[Title Page](#)[Abstract](#)[Introduction](#)[Conclusions](#)[References](#)[Tables](#)[Figures](#)[I◀](#)[▶I](#)[◀](#)[▶](#)[Back](#)[Close](#)[Full Screen / Esc](#)[Printer-friendly Version](#)[Interactive Discussion](#)

The maximum frequency of the dominant mode is reached for higher backscatter values for taiga than for tundra (Fig. 2) due to the typical higher contribution of vegetation to the backscatter. The backscatter distribution for non-water is comparably stable over time compared to the water surfaces represented in the minor mode (Fig. 3). Wind and rain can increase the roughness considerably what results in loss of the bimodal distribution and thus separability of the land cover classes. The overlap of the water backscatter with surrounding land cover in tundra is however in general larger than for boreal environment. Previous analyses has demonstrated classification accuracies of κ greater than 0.8 in the tundra-taiga transition zone (Bartsch et al., 2009).

Other thresholds have been tested in order to assess the impact of the predefinition of a universal threshold for separation of water surfaces from all other land cover. It can be assumed that values below the defined backscatter limit correspond to specular reflection from open, calm water outside of mountainous regions, during snow free period and without glaciation. More crucial is higher backscatter, which may correspond to mixed pixel response along the shorelines. This has been assessed by increases in 1 dB steps up to -13 dB and -12 dB.

2.3 Derivation of dynamics

A test for the presence of the bimodal distribution is necessary as a preprocessing step in order to account for roughness variation and loss of separability. A location specific reference distribution has been derived for each grid cell. It is extracted from the acquisition with the maximum inundation within the time series. The Pearson correlation between this reference and the backscatter distribution of each scene with full coverage has been extracted. Positive correlations indicate separability of a water class.

3 Results

The maximum water fraction per 0.5° cell reaches 35% in some areas but remains in general below 10% (Fig. 4). Variations occur in the region of the Ob-Estuary but also in basins within the tundra region. Thermokarst lakes “overflow” in early summer and slowly seasonally drain and/or vegetation emerges. This is exemplified in Fig. 5. This figure also demonstrates the persistence of lake ice on large lakes well into the summer.

More than 2300 samples (single scenes distributed over 133 cells; areas with coastal overlap are excluded) have been used for threshold testing for each of the summer periods (July and August) 2007 and 2008. 95% of samples show an increase of water fraction below 0.07 in case of threshold increase by 2 dB. There is a linear relationship between the fraction increase resulting from the different thresholds (Fig. 6b). An increase of 2 dB results in approximately two times the water fraction increase as for 1 dB. The majority of gained water fraction can be attributed to lake shores. An example is shown for a tundra region in Fig. 6c.

Figure 7 shows the water fraction for boreal as well as tundra environments over the summer period. Distinctive decrease occurs during short periods what can be attributed to wave action and precipitation. A bimodal distribution is only available for on average 40% (20–80%) of the acquisitions for areas with inundation fraction above 5%. The actual number of scenes during the two summer months varies between 20–30. This reduces the available samples from one every two/three days to approximately one scene per week.

There have been no meteorological stations with wind records for the analyses period as part of the WMO network within the transect available. The closest is Salehard (66.53° N, 66.53° E) west of the Ob estuary near to the Ob River. Data have been additionally processed for the covering 0.5 degree cell. Water fraction is expected to be also impacted by wave action on the stream. Wind data have been retrieved with respect to acquisition time. Wind speed is available every three hours. The closest

BGD

8, 8241–8268, 2011

High latitude wetland dynamics

A. Bartsch et al.

Title Page

Abstract

Introduction

Conclusions

References

Tables

Figures

◀

▶

◀

▶

Back

Close

Full Screen / Esc

Printer-friendly Version

Interactive Discussion



measurements (06:00 a.m. and 03:00 p.m.) have been extracted together with total daily precipitation. The time series is shown in Fig. 7. This specific analyses cell has a maximum water fraction of approximately 23%. High wind speed and precipitation can be observed during times with drop by often more than 50%. Such reductions due to weather occur over larger areas. It is observable during the same periods for most cells in each subregion (Figs. 7 and 8). The periods of unsuitable weather can exceed the theoretical weekly interval of data availability (scenes with bimodal distribution). Decadal updates are therefore suggested.

Grid cells with a maximum water fraction above 10% exhibit different behaviour for the tundra, taiga and floodplain when decadal periods are considered (Fig. 9). Open water fraction in the tundra biome increases up to 3% in 2007 and decreases by the same amount in 2008. Only very few grid cells have a high amount of lakes in the boreal part. There are some variations during the summer and also between the two years but on a very low level. A clear change over the summer for both years is only observable along the Ob floodplain and estuary. The inundated area is decreasing after the snowmelt related maximum extension.

4 Discussion

The impact of weather conditions on the applicability of C-band SAR for regular inundation monitoring are shown to be considerable although limited meteorological records are available for the region of interest. The exact precipitation timing is not retrievable from the meteorological stations records. Wind speed is also highly variable and not available for the exact timing of the satellite data acquisitions. The impact is nevertheless clearly visible in the classified datasets. A further constrain is the possible presence of ice on larger lakes until well into July. This needs to be taken into account for arctic regions.

In the present study the use of an empirical universal threshold has been tested. The characteristic bimodal distribution in regions with open water mixed with other land

BGD

8, 8241–8268, 2011

High latitude wetland dynamics

A. Bartsch et al.

Title Page

Abstract

Introduction

Conclusions

References

Tables

Figures

◀

▶

◀

▶

Back

Close

Full Screen / Esc

Printer-friendly Version

Interactive Discussion



High latitude wetland dynamics

A. Bartsch et al.

Title Page

Abstract

Introduction

Conclusions

References

Tables

Figures

◀

▶

◀

▶

Back

Close

Full Screen / Esc

Printer-friendly Version

Interactive Discussion



cover is similar for both tundra and taiga environment. The chosen threshold ranges between the lower limit of 3 to 4 standard deviations (Gaussian fit) of the main mode. The impact of an increase of the threshold is very low with up to 0.15 % for 1 dB and 0.25 % for 2 dB. This may be significant in case of applications where the exact borders of inundation are of relevance. Here, an efficient detection method for use across large regions is required. Weather conditions are more crucial for the detectability than the complexity of the classification approach since derived water fraction is often decreased by more than 50 %.

A pre-selection of the datasets is required. This might be done by use of meteorological data which are representative of the acquisition time. Such information is however unavailable over many regions. Backscatter statistics can be applied instead. The bimodal distribution is the major requirement when solely active microwave data are used. They may therefore be used as indicator in regions with a sufficient open water fraction.

The observed magnitude of inundation fraction agrees with previous analyses with coarser sensors. The study by Schroeder et al. (2010) which covers spring to end of July reports also fractions below 30 % for the chosen transect. Apart from the Ob floodplain, no changes over time are reported in Papa et al. (2008), especially none on Yamal. The SAR analyses shows that this region is characterized by seasonal changes which overlap with dynamics by thermokarst. Satellite data are often used to show longterm surface water variations (e.g. Smith et al., 2004). Wetland dynamics however need to be taken into account for long term analyses of permafrost degradation.

Methane emissions from wetlands scale linearly with the wetland fraction in the JULES model (Clark et al., 2011). It implements the parameterisation developed by Gedney et al. (2004):

$$F_w(\text{CH}_4) = k(\text{CH}_4) f_w C_s Q_{10}(T_{\text{soil}})^{(T_{\text{soil}} - T_0)/10} \quad (1)$$

where $F_w(\text{CH}_4)$ is the methane emission flux (in $\text{kg C m}^{-2} \text{s}^{-1}$), f_w is the wetland fraction, T_{soil} is the soil temperature (in K) averaged over the top 10 cm and $k(\text{CH}_4)$ is a

constant ($= 7.4 \times 10^{-12} \text{ s}^{-1}$). The temperature dependence is represented by a Q_{10} factor ($Q_{10}(T_0) = 3.7$ with $T_0 = 273.15 \text{ K}$). Soil carbon content (C_s) is used as there is a lack of global data on substrate availability. Gedney et al. (2004) assumed that only the fraction of the grid box where the water table was at or above the surface (i.e. f_w) resulted in net emission of CH_4 , otherwise methanotrophic bacteria in the aerobic soil completely oxidise all the CH_4 produced from the methanogenic bacteria. Wetland fraction of each grid box is a key term in the generation of methane from wetlands. This can either be derived within the hydrological scheme used in the land surface model, prescribed from analysis of separate data or a combination of the two approaches can be used. As such there is no minimum or threshold wetland fraction but there is clearly a value below which the emission flux would be insignificant in terms of its effect on atmospheric methane concentrations. Atmospheric measurements potentially provide a constraint on the minimum wetland fraction that should be represented in a wetland product. Gerilowski et al. (2011) are developing a successor to the Sciamachy instrument – the methane mapper (MAMAP). They considered a number of potential sources, including wetlands, which could be monitored by the MAMAP instrument. Gerilowski et al. (2011) defined an accumulation distance over which the emissions from diffuse sources (such as wetlands) would need to be integrated to give a measurable change in the atmospheric CH_4 column. They derived a value of 86 km for a strong summertime emission flux from wetlands of $200 \text{ mg CH}_4 \text{ m}^{-2} \text{ day}^{-1}$. Thus the sensitivity of satellite estimates of atmospheric methane concentration does not currently impose a tight constraint on the required accuracy of a wetland product.

Data on wetland extent are also important in relation to the thawing of permafrost in a warming climate. Permafrost, defined as ground (soil or rock) that remains at or below 0°C for at least two consecutive years. It accounts for approximately 22% of the exposed land area in the Northern Hemisphere and is globally a significant store of organic carbon (Schuur et al., 2008). O'Connor et al. (2010) considered the water saturation status of the thawing permafrost to be the most important factor in determining whether the release of the frozen carbon occurred as CO_2 or CH_4 . Depending on

BGD

8, 8241–8268, 2011

High latitude wetland dynamics

A. Bartsch et al.

Title Page

Abstract

Introduction

Conclusions

References

Tables

Figures

◀

▶

◀

▶

Back

Close

Full Screen / Esc

Printer-friendly Version

Interactive Discussion



the conditions, thawing may lead to enhanced soil drainage and therefore a lowering of the water table (i.e. more CO₂), or the opposite, whereby landscape collapse leads to impeded drainage and a raised water table (i.e. more CH₄). The evolution of areas of saturation also exerts a strong control on the exchanges of heat and moisture between the land surface and the atmosphere, which are of critical importance to climate models.

5 Conclusions

A major known problem for application of SAR data for inundation monitoring is data availability and the used wavelengths. A series of European satellites (ERS, ENVISAT and the upcoming Sentinel 1) have SAR instruments operating in C-band. The suitability of data acquired at this wavelength is limited due to sensitivity to roughness changes on water surfaces. The major advantage over L-band sensors is the coverage and continuity what is important for monitoring purposes. A region with comparably good data availability in the past and importance regarding wetland dynamics has been chosen in order to investigate further constraints. Especially the issue of classification method and impact of weather phenomena has been studied.

Although SAR data are independent of cloudiness and daylight availability, weather has a significant effect. More than on average 60% of the data are affected in tundra and taiga areas of Western Siberia. Detection results cannot be used on a single day basis. Update intervals need to be chosen depending on the possible persistence of rainy and windy weather conditions and the actual sampling interval. A minimum of 10 days is suggested for the Western Siberia region for the summer periods 2007 and 2008. Such intervals are shorter than in previously applied satellite data products in climate models (Ringeval et al., 2010, 2011; Riley et al., 2011).

The actual methods of classification are robust in case of separability of the water class from other land cover. A universal threshold can be used as long as the bimodal backscatter distribution is maintained. Variations in the threshold do not significantly

BGD

8, 8241–8268, 2011

High latitude wetland dynamics

A. Bartsch et al.

Title Page

Abstract

Introduction

Conclusions

References

Tables

Figures

◀

▶

◀

▶

Back

Close

Full Screen / Esc

Printer-friendly Version

Interactive Discussion



impact the resulting water fraction. The increase is below 1%. Locations which are mostly affected are lake rims.

General trends in floodplains can be still followed if maximum fraction values within predefined periods are used. Seasonal changes can be also observed in the boreal and tundra biome but on a lower level. There are single lakes which drain and refill especially in tundra regions where seasonal overflowing of thermokarst lakes occurs. This seasonal behaviour needs to be considered when remotely sensed data are used for analyses of thermokarst as part of permafrost monitoring schemes.

The effects of wetland features on fluxes generally occur at scales much smaller than those of a typical model grid box and as such have to be parameterised. The development and testing of model parameterisations, and the long-term monitoring of these changes in the environment, require information about the sub-grid scale distribution of wetlands over large areas, which is exactly the sort of information that a SAR product could provide. As part of the space component of the Global Monitoring for Environment and Security (GMES) programme, the European Union (EU) and the European Space Agency (ESA) are preparing the next generation of imaging Synthetic Aperture Radars (SARs): the Sentinel-1 mission. The Sentinel-1 satellites will provide all-weather, day-and-night observations (Attema et al., 2007). In order to fulfil user requirements for operationally sustainable services, the mission is based – in contrast to the ERS-1, ERS-2 and ENVISAT missions – upon an operational concept (Attema, 2005). This would allow for frequent mapping of inundation dynamics.

Acknowledgements. This study has been carried out in relation to the ALANIS-Methane project which is funded by the European Space Agency (ESA) Support to Science Element (STSE) program (ESRIN Contr. No. 4000100647/10/I-LG) and coordinated by CEH, UK. It further contributes to the PERMAFROST project which is funded by ESA's Data User Element (DUE) program as a component of the Earth Observation Envelope Program (EOEP) (ESRIN Contr. No. 22185/09/I-OL) and coordinated by TU Wien. A. Bartsch has been recipient of a fellowship by the Austrian Science Fund (V150-N21).

BGD

8, 8241–8268, 2011

High latitude wetland dynamics

A. Bartsch et al.

Title Page

Abstract

Introduction

Conclusions

References

Tables

Figures

◀

▶

◀

▶

Back

Close

Full Screen / Esc

Printer-friendly Version

Interactive Discussion



References

- Attema, E.: Mission Requirement Document for the European Radar Observatory Sentinel-1 (Mission Requirement Specification), European Space Agency, 2005. 8255
- Attema, E., Bargellini, P., Edwards, P., Levrini, G., Lokas, S., and Moeller, L.: Sentinel-1 – the radar mission for GMES operational land and sea services, *ESA Bulletin*, 131, 10–17, 2007. 8245, 8255
- Bartsch, A.: Ten Years of SeaWinds on QuikSCAT for Snow Applications, *Remote Sensing*, 2, 1142–1156, 2010. 8244
- Bartsch, A., Pathe, C., Wagner, W., and Scipal, K.: Detection of Permanent Open Water Surfaces in Central Siberia with ENVISAT ASAR Wide Swath Data with Special Emphasis on the Estimation of Methane Fluxes from Tundra Wetlands, *Hydrol. Res.*, 39, 89–100, 2008. 8244, 8245, 8246
- Bartsch, A., Wagner, W., Scipal, K., Pathe, C., Sabel, D., and Wolski, P.: Global Monitoring of Wetlands – the Value of ENVISAT ASAR Global Mode, *J. Environ. Manage.*, 90, 2226–2233, 2009. 8246, 8248, 8249
- Clark, D. B., Mercado, L. M., Sitch, S., Jones, C. D., Gedney, N., Best, M. J., Pryor, M., Rooney, G. G., Essery, R. L. H., Blyth, E., Boucher, O., Harding, R. J., and Cox, P. M.: The Joint UK Land Environment Simulator (JULES), Model description – Part 2: Carbon fluxes and vegetation, *Geosci. Model Dev. Discuss.*, 4, 641–688, doi:10.5194/gmdd-4-641-2011, 2011. 8243, 8252
- Denman, K. L., Brasseur, G., Chidthaisong, A., Ciais, P., Cox, P., Dickinson, R., Hauglustaine, D., Heinze, C., Holland, E., Jacob, D., Lohmann, U., Ramachandran, S., da Silva Dias, P., Wofsy, S., and Zhang, X.: Couplings Between Changes in the Climate System and Biogeochemistry, in: *Climate Change 2007: The Physical Science Basis. Contribution of Working Group I to the Fourth Assessment Report of the Intergovernmental Panel on Climate Change*, edited by: Solomon, S., Qin, D., Manning, M., Chen, Z., Marquis, M., Averyt, K., Tignor, M., and Miller, H., Cambridge University Press, Cambridge, United Kingdom and New York, NY, USA, 2007. 8243
- Duguay, C. R., Pultz, T. J., Lafleur, P. M., and Drai, D.: RADARSAT Backscatter Characteristics of Ice Growing on Shallow Sub-Arctic Lakes, Churchill, Manitoba, Canada, *Hydrol. Process.*, 16, 1631–1644, 2002. 8246
- Frey, K. and Smith, L. C.: How Well Do We Know Northern Land Cover? Comparison of

BGD

8, 8241–8268, 2011

High latitude wetland dynamics

A. Bartsch et al.

Title Page

Abstract

Introduction

Conclusions

References

Tables

Figures

◀

▶

◀

▶

Back

Close

Full Screen / Esc

Printer-friendly Version

Interactive Discussion



- Four Global Vegetation and Wetland Products with a New Ground-Truth Database for West Siberia, *Global Biogeochem. Cy.*, 21, GB1016, doi:10.1029/2006GB002706, 2007. 8244
- Gedney, N., Cox, P. M., and Huntingford, C.: Climate feedback from wetland methane emissions, *Geophys. Res. Lett.*, 31, L20503, doi:10.1029/2004GL020919, 2004. 8252, 8253
- 5 Gerilowski, K., Tretner, A., Krings, T., Buchwitz, M., Bertagnolio, P. P., Belemezov, F., Erzinger, J., Burrows, J. P., and Bovensmann, H.: MAMAP – a new spectrometer system for column-averaged methane and carbon dioxide observations from aircraft: instrument description and performance analysis, *Atmos. Meas. Tech.*, 4, 215–243, doi:10.5194/amt-4-215-2011, 2011. 8253
- 10 Keddy, P. A. and Fraser, L. H.: *The World's Largest Wetlands: Ecology and Conservation*, chap. Introduction: big is beautiful, Cambridge University Press, 1–10, 2005. 8246
- Lehner, B. and Döll, P.: Development and Validation of a Global Database of Lakes, Reservoirs and Wetlands, *J. Hydrol.*, 296, 1–22, 2004. 8244
- Matgen, P., Hostache, R., Schumann, G., Pfister, L., Hoffmann, L., and Savenije, H.: Towards an automated SAR-based flood monitoring system: Lessons learned from two case studies, *Phys. Chem. Earth*, 36, 241–252, 2011. 8245, 8248
- 15 Matthews, E. and Fung, I.: Methane Emission from Natural Wetlands: Global Distribution, Area, and Environmental Characteristics of Sources, *Global Biochem. Cy.*, 1, 61–86, 1987. 8244
- Mikaloff Fletcher, S. E., Tans, P. P., Bruhwiler, L. M., Miller, J. B., and Heimann, M.: CH₄ sources estimated from atmospheric observations of CH₄ and its ¹³C/¹²C isotopic ratios: 1. Inverse modelling of source processes, *Global Biogeochem. Cy.*, 18, GB4004, doi:10.1029/2004GB002223, 2004. 8243
- 20 O'Connor, F. M., Boucher, Gedney, N., Jones, C. D., Folberth, G. A., Coppell, R., Friedlingstein, P., Collins, W., Chappellaz, J., Ridley, J., and Johnson, C. E.: The possible role of wetlands, permafrost and methane hydrates in the methane cycle under future climate change: A review, *Rev. Geophys.*, 48, RG4005, doi:10.1029/2010RG000326, 2010. 8253
- 25 Papa, F., Prigent, C., and Rossow, W. B.: Monitoring Flood and Discharge Variations in the Large Siberian Rivers From a Multi-Satellite Technique, *Surv. Geophys.*, 29, 297–317, 2008. 8252
- 30 Petrescu, A., van Beek, L., van Huissteden, J., Prigent, C., Sachs, T., Corradi, C. A. R., Parmentier, F. J. W., and Dolman, A. J.: Modeling regional to global CH₄ emissions of boreal and arctic wetlands, *Global Biogeochem. Cy.*, 24, GB4009, doi:10.1029/2009GB003610, 2010. 8243

High latitude wetland dynamics

A. Bartsch et al.

Title Page

Abstract

Introduction

Conclusions

References

Tables

Figures

◀

▶

◀

▶

Back

Close

Full Screen / Esc

Printer-friendly Version

Interactive Discussion



- Prigent, C., Matthews, E., Aires, F., and Rossow, W. B.: Remote Sensing of Global Wetland Dynamics with Multiple Satellite Data Sets, *Geophys. Res. Lett.*, 28, 4631–4634, 2001. 8244
- Prigent, C., Papa, F., Aires, F., Rossow, W. B., and Matthews, E.: Global Inundation Dynamics Inferred from Multiple Satellite Observations, 1993–2000, *J. Geophys. Res.*, 112, D12107, doi:10.1029/2006JD007847, 2007. 8244
- Riley, W. J., Subin, Z. M., Lawrence, D. M., Swenson, S. C., Torn, M. S., Meng, L., Mahowald, N. M., and Hess, P.: Barriers to predicting changes in global terrestrial methane fluxes: analyses using CLM4Me, a methane biogeochemistry model integrated in CESM, *Biogeosciences*, 8, 1925–1953, doi:10.5194/bg-8-1925-2011, 2011. 8243, 8244, 8254
- Ringeval, B., de Noblet-Ducoudre, N., Ciais, P., Bousquet, P., Prigent, C., Papa, F., and Rossow, W. B.: An Attempt to Quantify the Impact of Changes in Wetland Extent on Methane Emissions on the Seasonal and Interannual Time Scales, *Global Biogeochem. Cy.*, 24, GB2003, doi:10.1029/2008GB003354, 2010. 8243, 8244, 8246, 8254
- Ringeval, B., Friedlingstein, P., Koven, C., Ciais, P., de Noblet-Ducoudré, N., Decharme, B., and Cadule, P.: Climate-CH₄ feedback from wetlands and its interaction with the climate-CO₂ feedback, *Biogeosciences Discuss.*, 8, 3203–3251, doi:10.5194/bgd-8-3203-2011, 2011. 8243, 8244, 8254
- Sabel, D., Bartalis, Z., Wagner, W., Doubkova, M., and Klein, J.-P.: Development of a Global Backscatter Model in support to the Sentinel-1 mission design, *Remote Sens. Environ.*, in review, 2011. 8247
- Schneising, O., Buchwitz, M., Reuter, M., Heymann, J., Bovensmann, H., and Burrows, J. P.: Long-term analysis of carbon dioxide and methane column-averaged mole fractions retrieved from SCIAMACHY, *Atmos. Chem. Phys.*, 11, 2863–2880, doi:10.5194/acp-11-2863-2011, 2011. 8246
- Schroeder, R., Rawlins, M. A., McDonald, K. C., Podest, E., Zimmermann, R., and Kueppers, M.: Satellite microwave remote sensing of North Eurasian inundation dynamics: development of coarse-resolution products and comparison with high-resolution synthetic aperture radar data, *Environ. Res. Lett.*, 5, 015003, doi:10.1088/1748-9326/5/1/015003, 2010. 8244, 8248, 8252
- Schuur, E., Bockheim, J., Canadell, J., Euskirchen, E., Field, C. B., Goryachkin, S. V., Hagemann, S., Kuhry, P., Lafleur, P., Lee, H., Mazhitova, G., Nelson, F. E., Rinke, A., Romanovsky, V., Shiklomanov, N., Tarnocai, C., Venevsky, S., Vogel, J. G., and Zimov, S. A.: Vulnerability of permafrost carbon to climate change: Implications for the global carbon cycle, *BioScience*,

BGD

8, 8241–8268, 2011

High latitude wetland dynamics

A. Bartsch et al.

Title Page

Abstract

Introduction

Conclusions

References

Tables

Figures

◀

▶

◀

▶

Back

Close

Full Screen / Esc

Printer-friendly Version

Interactive Discussion



High latitude wetland dynamics

A. Bartsch et al.

Title Page

Abstract

Introduction

Conclusions

References

Tables

Figures

◀

▶

◀

▶

Back

Close

Full Screen / Esc

Printer-friendly Version

Interactive Discussion



58, 701–714, 2008. 8243, 8253

Smith, L. C., MacDonald, G. M., Velichko, A. A., Beilman, D. W., Borisova, O. K., Frey, K. E., Kremenetski, K. V., and Sheng, Y.: Siberian Peatlands a Net Carbon Sink and Global Methane Source Since the Eearly Holocene, *Science*, 303, 353–356, 2004. 8252

5 Walter, B. P., Heimann, M., and Matthews, E.: Modeling modern methane emissions from natural wetlands 1. Model description and results, *J. Geophys. Res.*, 106, 34189–34206, 2001. 8243

10 Wania, R., Ross, I., and Prentice, I.: Integrating peatlands and permafrost into a dynamic global vegetation model: 1. Evaluation and sensitivity of physical land surface processes, *Global Biogeochem. Cy.*, 23, GB3014, doi:10.1029/2008GB003412, 2009a. 8243

Wania, R., Ross, I., and Prentice, I. C.: Integrating peatlands and permafrost into a dynamic global vegetation model: 2. Evaluation and sensitivity of vegetation and carbon cycle processes, *Global Biogeochem. Cy.*, 23, GB3015, doi:10.1029/2008GB003413, 2009b. 8243

15 Whitcomb, J., Moghaddam, M., McDonald, K., Kellndorfer, J., and Podest, E.: Mapping vegetated wetlands of Alaska using L-band radar satellite imagery, *Can. J. Remote Sens.*, 35, 54–72, 2009. 8248

Wuebbles, D. J. and Hayhoe, K.: Atmospheric methane and global change, *Earth Sci. Rev.*, 57, 177–210, 2002. 8243

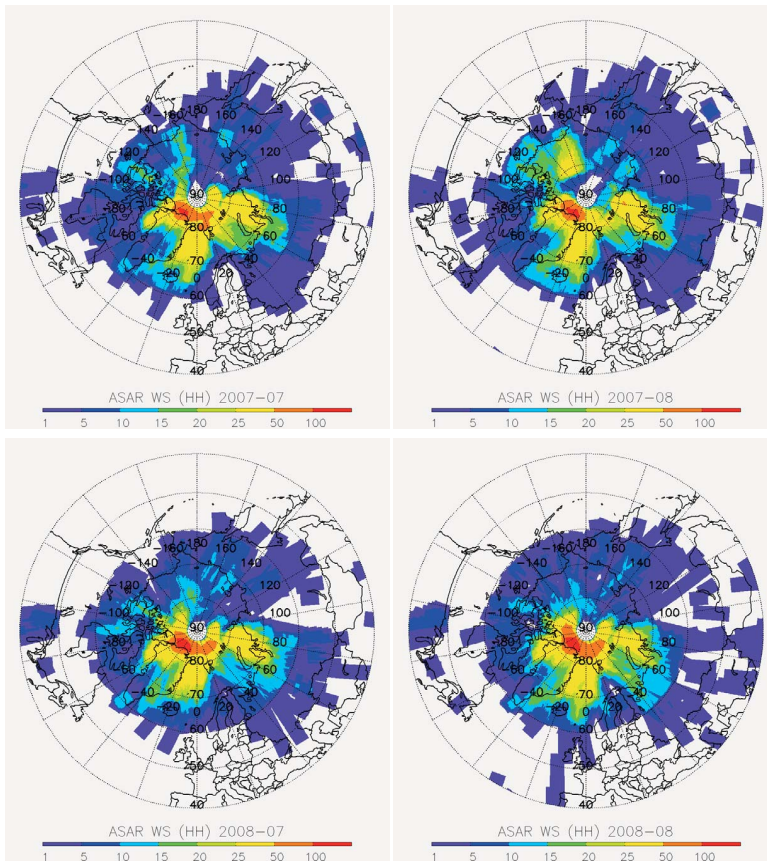


Fig. 1. ASAR WS data availability for HH polarisation at high latitudes: July and August 2007/2008.

High latitude wetland dynamics

A. Bartsch et al.

Title Page

Abstract Introduction

Conclusions References

Tables Figures

◀ ▶

◀ ▶

Back Close

Full Screen / Esc

Printer-friendly Version

Interactive Discussion



High latitude wetland dynamics

A. Bartsch et al.

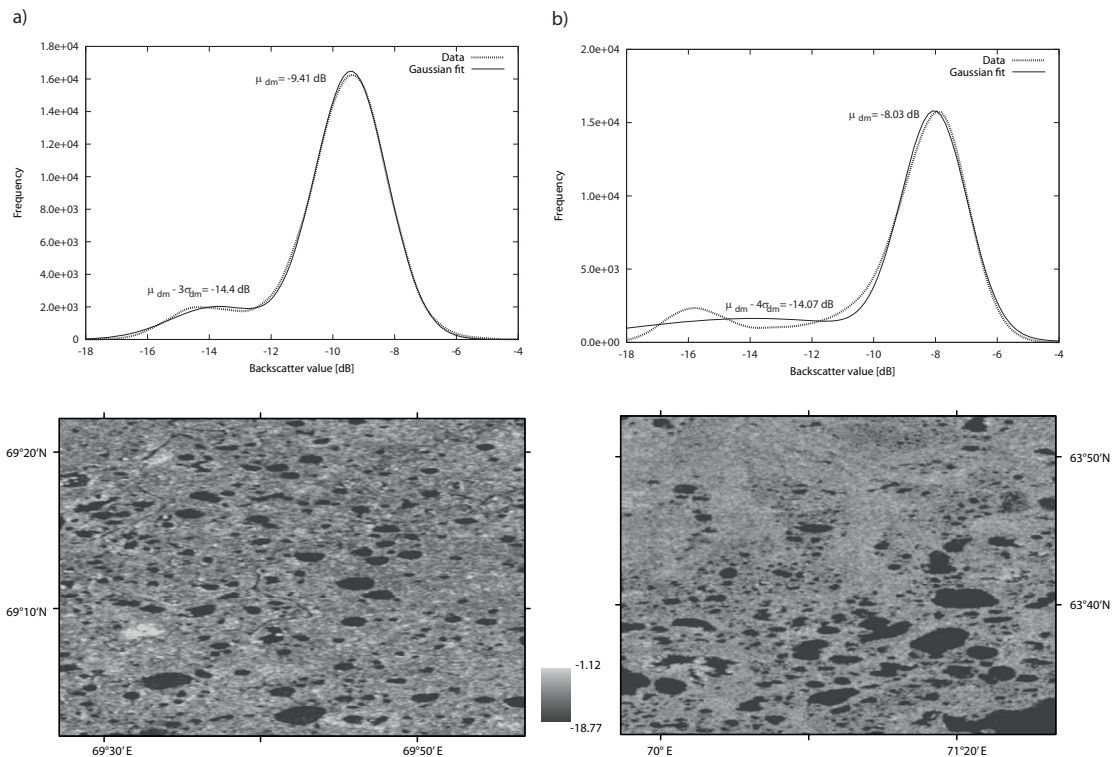


Fig. 2. Examples from summer 2007: **(a)** backscatter value distribution and corresponding ASAR WS backscatter images for **(a)** tundra (20 August 2007) and **(b)** taiga (12 July 2007).

Title Page

Abstract

Introduction

Conclusions

References

Tables

Figures

◀

▶

◀

▶

Back

Close

Full Screen / Esc

Printer-friendly Version

Interactive Discussion



High latitude wetland dynamics

A. Bartsch et al.

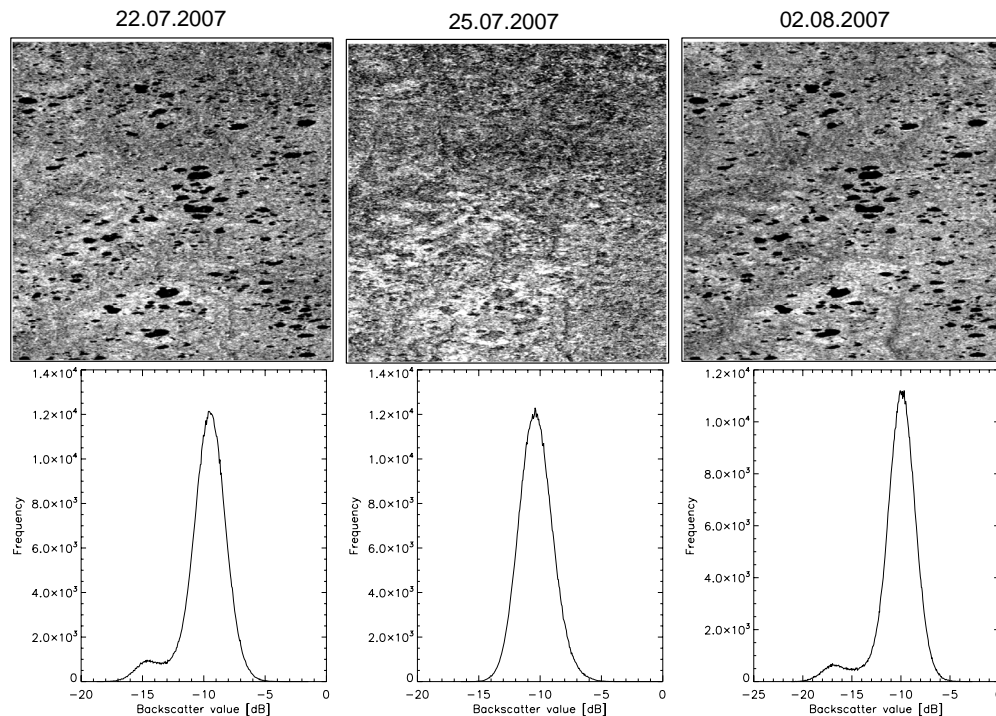


Fig. 3. Backscatter time series example for loss of bimodal distribution over tundra: top normalized backscatter images, bottom: histograms of backscatter distribution [dB].

Title Page

Abstract

Introduction

Conclusions

References

Tables

Figures

◀

▶

◀

▶

Back

Close

Full Screen / Esc

Printer-friendly Version

Interactive Discussion



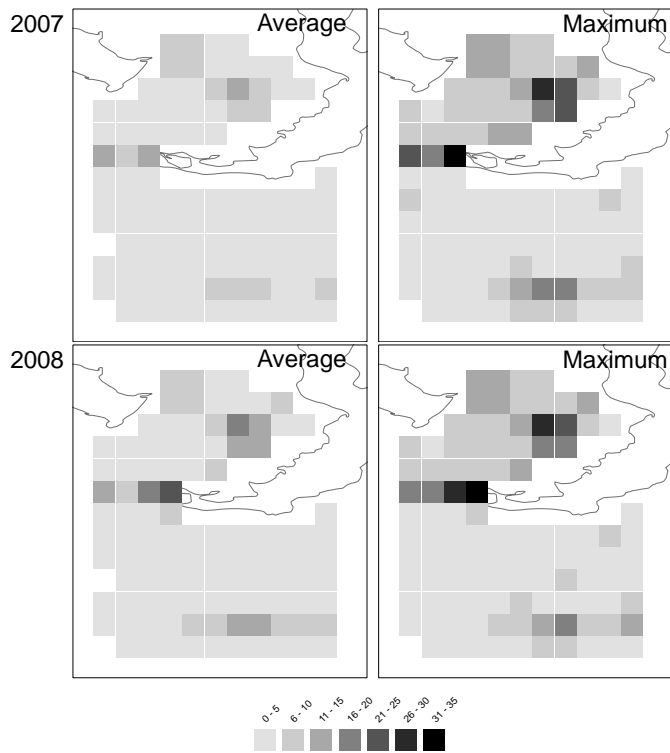


Fig. 4. Water fraction maps from ASAR WS in July/August 2007 and 2008: (left) average and (right) maximum.

High latitude wetland dynamics

A. Bartsch et al.

Title Page

Abstract Introduction

Conclusions References

Tables Figures

◀ ▶

◀ ▶

Back Close

Full Screen / Esc

Printer-friendly Version

Interactive Discussion



High latitude wetland dynamics

A. Bartsch et al.

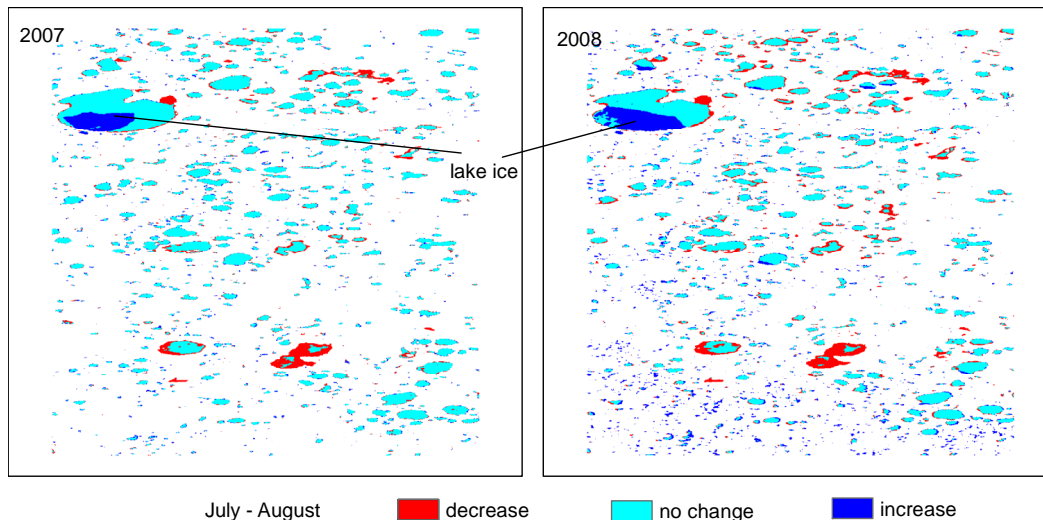


Fig. 5. Example for seasonal changes of open water extent in tundra (within a 0.5 degree cell): left – 7 September 2007 and 28 August 2007, right – 6 July 2008 and 21 August 2008.

Title Page

Abstract

Introduction

Conclusions

References

Tables

Figures

◀

▶

◀

▶

Back

Close

Full Screen / Esc

Printer-friendly Version

Interactive Discussion



High latitude wetland dynamics

A. Bartsch et al.

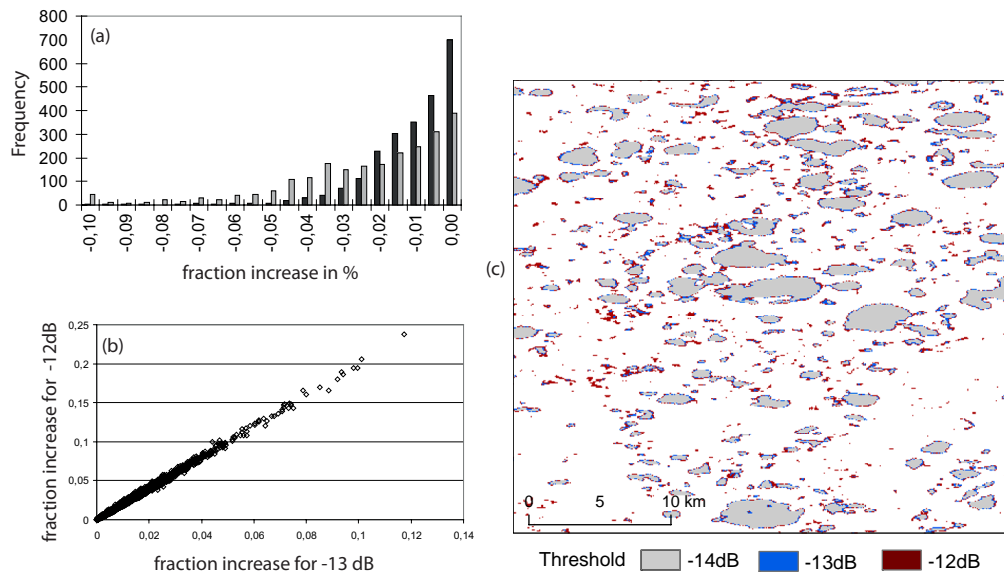


Fig. 6. Differences of water fraction for different thresholds: **(a)** histogram with black – 1 dB increase, grey – 2 dB increase, **(b)** scatterplot of fraction difference in comparison with a –14 dB threshold and **(c)** example of classification results differences in tundra.

Discussion Paper | Discussion Paper | Discussion Paper | Discussion Paper | Discussion Paper

Title Page

Abstract

Introduction

Conclusions

References

Tables

Figures

◀

▶

◀

▶

Back

Close

Full Screen / Esc

Printer-friendly Version

Interactive Discussion



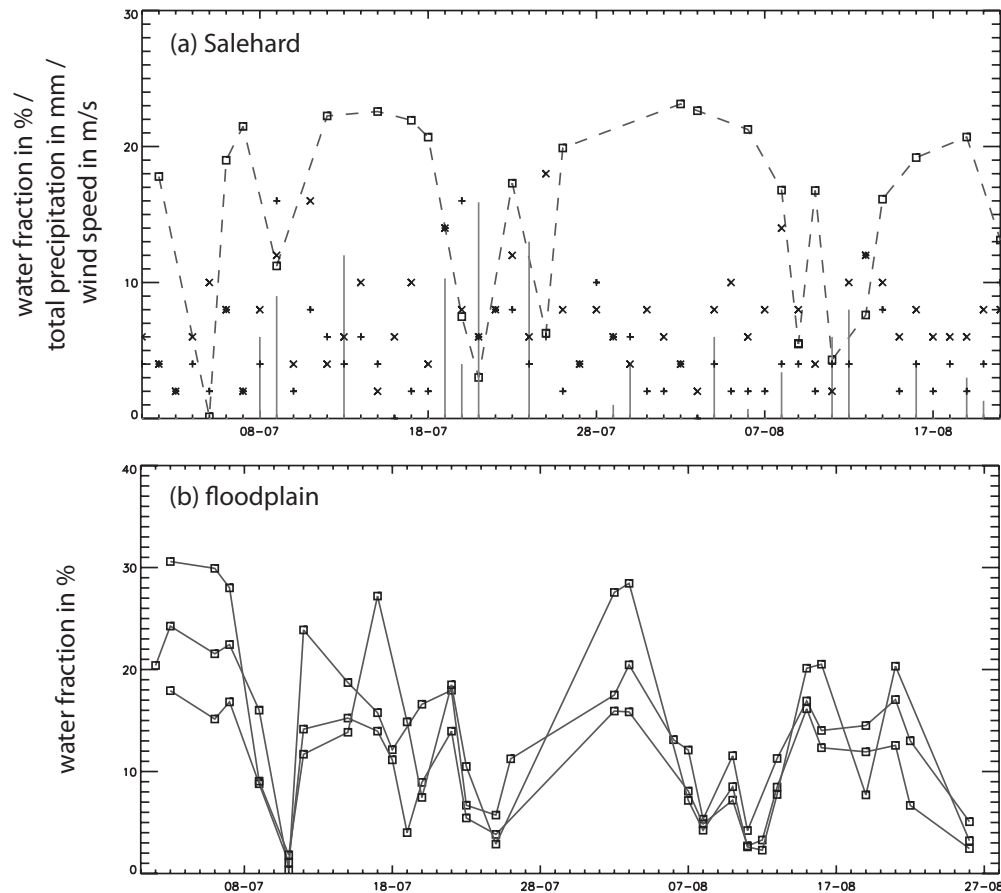


Fig. 7. Variation of water fraction from ASAR WS in summer 2007 with minimum 10%: **(a)** the region of Salehard in % (squares), wind speed from meteorological data (+06:00 a.m., ×03:00 p.m.) in m s^{-1} , total daily precipitation in mm (vertical bars) **(b)** cells of the floodplain (66–67° N).

[Title Page](#)
[Abstract](#)
[Introduction](#)
[Conclusions](#)
[References](#)
[Tables](#)
[Figures](#)
[◀](#)
[▶](#)
[◀](#)
[▶](#)
[Back](#)
[Close](#)
[Full Screen / Esc](#)
[Printer-friendly Version](#)
[Interactive Discussion](#)

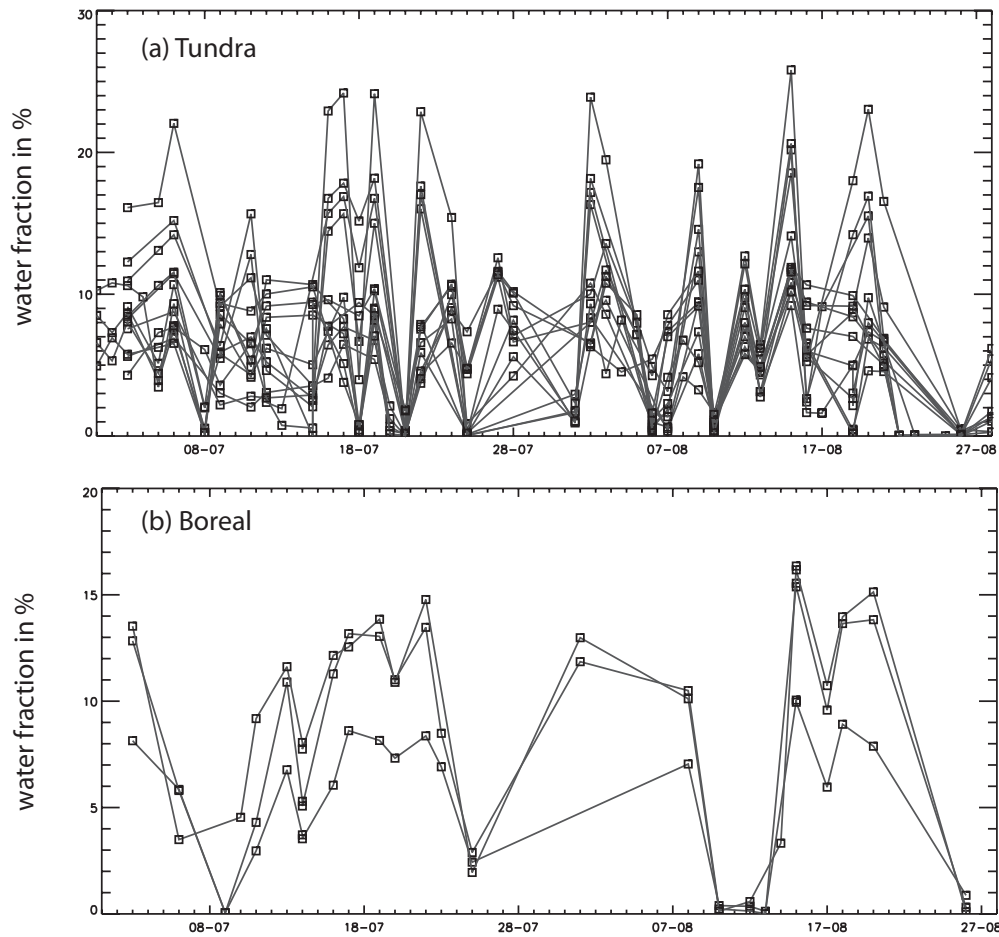



Fig. 8. Variation of water fraction from ASAR WS in summer 2007 with minimum 10%: **(a)** all cells north of 67° N, **(b)** all cells south of 66° N.

Title Page

Abstract Introduction

Conclusions References

Tables Figures

◀ ▶

◀ ▶

Back Close

Full Screen / Esc

Printer-friendly Version

Interactive Discussion



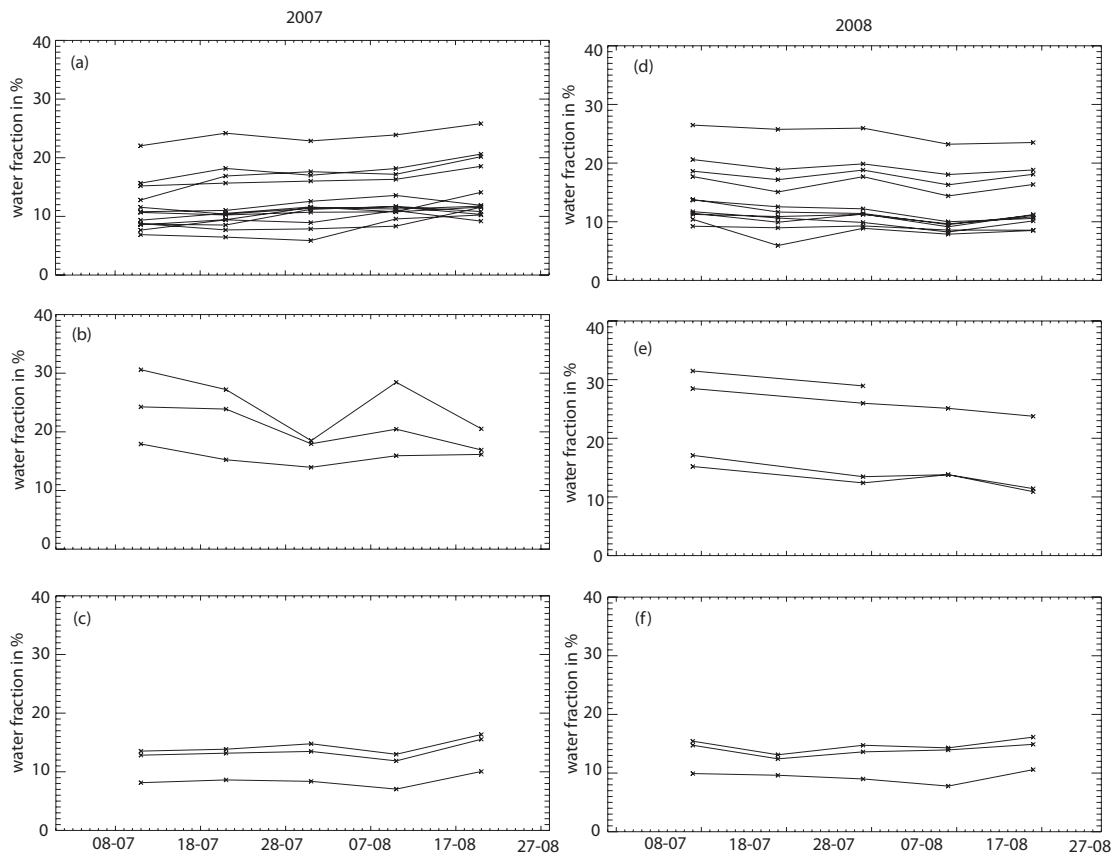


Fig. 9. Decadal maximum of grid cells >10% water fraction from ASAR WS in summer 2007 for **(a)** all cells north of 67° N, **(b)** cells of the floodplain, **(c)** all cells south of 66° N; **(d-f)** 2008, respectively.

[Title Page](#)

[Abstract](#) [Introduction](#)

[Conclusions](#) [References](#)

[Tables](#) [Figures](#)

[I ◀](#) [▶ I](#)

[◀](#) [▶](#)

[Back](#) [Close](#)

[Full Screen / Esc](#)

[Printer-friendly Version](#)

[Interactive Discussion](#)

